

The effect of ripple types on cross-shore

S. R. Kularatne et al.

This discussion paper is/has been under review for the journal Earth Surface Dynamics (ESurD). Please refer to the corresponding final paper in ESurf if available.

The effect of ripple types on cross-shore suspended sediment flux

S. R. Kularatne^{1,†}, J. Doucette^{2,*}, and C. B. Pattiaratchi¹

¹School of Civil, Environmental and Mining Engineering and UWA Oceans Institute, CRAWLEY WA 6009, Australia

²School of Earth and Geographical Sciences, The University of Western Australia, 35 Stirling Highway, Crawley, WA 6009, Australia

*now at: GHD Ltd, 6705 Millcreek Drive Unit 1 Mississauga ON L5N 5M4, Canada

†deceased

Received: 8 January 2014 – Accepted: 23 January 2014 – Published: 7 April 2014

Correspondence to: C. B. Pattiaratchi (chari.pattiaratchi@uwa.edu.au)

Published by Copernicus Publications on behalf of the European Geosciences Union.

Title Page

Abstract Introduction

Conclusions References

Tables Figures

◀ ▶

◀ ▶

Back Close

Full Screen / Esc

Printer-friendly Version

Interactive Discussion



Abstract

Field measurements, collected at several low energy, microtidal beaches in south-western Australia were used to study the cross-shore transport and sediment resuspension over different sand ripple types. The measurements included simultaneous records of the water surface elevation, cross-shore current velocity, and suspended sediment concentration, as well as free diver measurements of the ripple dimensions. The observed ripples were classified according to their geometry and sediment suspension patterns into six categories: flat bed, post-vortex ripples, two-dimensional (2-D) ripples, two/three-dimensional (2-D/3-D) ripples, three-dimensional (3-D) ripples, and cross ripples. Flat bed conditions were observed under the highest flow mobility numbers. Post-vortex ripples were observed under slightly lower mobility numbers. The other ripple types occurred under low mobility numbers, with no significant difference in the mobility number among them. Two-dimensional ripples were observed more than the other ripple types in the presence of coarse grains. The suspended sediment concentration at ~ 0.05 m above the bed was greater over steep ripples. The net cross-shore suspended sediment flux close to the seabed (at ~ 0.05 m) in the swell frequency band varied over the different ripples types: onshore over a flat bed, offshore over post-vortex ripples, onshore over 2-D and 2-D/3-D ripples, and offshore over 3-D ripples. The suspended sediment flux direction over the cross ripples varied between onshore and offshore.

1 Introduction

The presence of wave-induced ripples on the seabed greatly impacts the sediment resuspension and transport in nearshore environments (Osborne and Greenwood, 1992b; Brander and Greenwood, 1993; Davidson et al., 1993; Osborne and Vincent, 1993, 1996; Masselink and Pattiaratchi, 2000; Masselink et al., 2007; Hurther and Thorne, 2011). Although bed load transport is the main transport mode over a flat bed

ESURFD

2, 215–254, 2014

The effect of ripple types on cross-shore

S. R. Kularatne et al.

Title Page

Abstract

Introduction

Conclusions

References

Tables

Figures

◀

▶

◀

▶

Back

Close

Full Screen / Esc

Printer-friendly Version

Interactive Discussion



(sheet flow), suspended load transport is dominant over rippled beds (Brenninkmeyer, 1976; Bailard and Inman, 1979; Nielsen, 1979; Hanes, 1988; Sternberg et al., 1989; Aagaard et al., 2013).

Over a flat bed, sediment resuspension mainly occurs as a diffusive process; over ripples, it is more convective, with the sand-laden separation vortices formed in the leeside of ripples being ejected up into the water column as waves pass (Lee and Hanes, 1996). These vortices, however, do not always appear with the presence of ripples, as the vortex formation depends on the ripple geometry. Vortex formation can be seen over steep ripples at regular intervals when the ratio between the ripple height (η) and ripple length (λ) – ripple steepness (η/λ) – is greater than 0.1. These ripples are named vortex ripples (Clifton and Dingler, 1984). Consistent vortex formation has not been observed over ripples when the steepness is < 0.1 ; these ripples are called post-vortex ripples (Clifton and Dingler, 1984).

Increased suspended sediment concentrations have been observed high in the water column when vortex ripples are present (Vincent et al., 1991; Osborne and Greenwood, 1993; Osborne and Vincent, 1996) because the vortices eject sand up into the water column. The vertical length scale of the suspended sediment concentration profiles is a strong function of the ripple height (Nielsen, 1984).

Cross-shore suspended sediment flux over a flat bed under shoaling, non-breaking, incident (swell, wind) waves has often been observed in the onshore direction (Osborne and Greenwood, 1992b; Davidson et al., 1993; Masselink et al., 2007; Hurther and Thorne, 2011). Huntley and Hanes (1987) first highlighted this trend and attributed it to the increased velocity skewness that occurs with shoaling waves (Osborne and Greenwood, 1992b). Many researchers have also observed offshore suspended sediment flux in the swell frequency band (Osborne and Greenwood, 1992b; Davidson et al., 1993; Masselink and Pattiaratchi, 2000); the presence of ripples is considered the most likely cause for this reversal in the suspended sediment flux direction (Osborne and Greenwood, 1992b; Davidson et al., 1993).

The effect of ripple types on cross-shoreS. R. Kularatne et al.

Title Page

Abstract

Introduction

Conclusions

References

Tables

Figures

◀

▶

◀

▶

Back

Close

Full Screen / Esc

Printer-friendly Version

Interactive Discussion



The effect of ripple types on cross-shore

S. R. Kularatne et al.

Title Page

Abstract

Introduction

Conclusions

References

Tables

Figures

◀

▶

◀

▶

Back

Close

Full Screen / Esc

Printer-friendly Version

Interactive Discussion



The timing of sediment suspension in relation to the cross-shore velocity can change depending on the ripple geometry (Osborne and Vincent, 1993, 1996), which can cause the suspended sediment transport in the swell frequency band to alternate direction between onshore and offshore. Inman and Bowen (1963) first described a mechanism for seaward suspended sediment flux in the swell frequency band over a rippled bed. They described the resuspension and transport process over steep vortex ripples as follows: (1) when a skewed wave propagates over vortex ripples, a vortex is formed on the ripple's leeside during the strong onshore phase, and remains trapped until the flow reverses; (2) during the weaker offshore phase, the sand-laden vortex is released, ejected into the water column, and transported seaward.

Offshore sediment flux in the swell frequency band has sometimes been observed over gentle post-vortex ripples (Osborne and Greenwood, 1992b; Brander and Greenwood, 1993) and onshore flux has been measured over steep ripples (Osborne and Greenwood, 1992b). Davidson et al. (1993) observed offshore flux due to swell waves over a rippled bed, but the ripple geometry was not measured; thus it was unclear whether the ripples were vortex or post-vortex.

The above observations suggest the direction of suspended sediment flux in the swell frequency band could be a function of the ripple geometry, and thus could vary over different ripple types. Few detailed studies of cross-shore sediment flux over different ripple types have been undertaken (Brander and Greenwood, 1993; Osborne and Vincent, 1993, 1996), yet they are essential to gain an understanding of sediment resuspension and transport processes in nearshore environments.

This paper presents the results of measurements (water surface elevation, cross-shore current velocity, and suspended sediment concentration) collected under shoaling waves over different ripple types at low energy, microtidal beaches in south-western Australia. Doucette (2000) first presented these data, which focused on the ripple geometry; however, we examined the effect of ripples on cross-shore suspended sediment flux. The changes in the bed morphology were also observed concurrently with the ripple measurements. The cross-shore suspended sediment flux in the frequency

domain for each data set was studied to identify any trends with the ripple types. The results of further cross-spectral and cross-correlation analyses are then presented to determine why the suspended sediment flux over the different ripple types had different directions and magnitudes.

2 Methodology

2.1 Field sites

Field measurements were collected from 15 sandy, micro-tidal, low energy beaches in south-western Australia between 31 October 1997 and 2 April 1998 (Fig. 1; see also Doucette, 2000). The measurements were obtained from discrete cross-shore locations in the nearshore and provided a total of 60 data sets (ref. Table 1 in Doucette, 2000). The mean sand grain size (d_{50}) at the field sites varied between 0.14 and 0.54 mm. More details about the field sites can be found in Doucette (2000).

2.2 Data collection

The instruments used to collect the data included a Marsh-McBirney Inc. 511 electromagnetic current meter, two D & A optical backscatter sensors, and a pressure sensor to measure the two-dimensional horizontal components of the cross-shore current velocity, suspended sediment concentration, and water surface elevation, respectively. The instruments were mounted on a portable frame (see Fig. 2 in Doucette, 2000), with the current meter placed 0.25 m above the bed, the optical backscatter sensors placed 0.05 m and 0.13 m above the bed, and the pressure sensor placed 0.05 m above the bed. The duration of each measurement was at least 17 min (4096 data points at a frequency of 4 Hz). During each deployment, a free diver measured the ripple height and length with a ruler. Further details can be found in Doucette (2000).

The effect of ripple types on cross-shore

S. R. Kularatne et al.

Title Page

Abstract

Introduction

Conclusions

References

Tables

Figures

◀

▶

◀

▶

Back

Close

Full Screen / Esc

Printer-friendly Version

Interactive Discussion



2.3 Data analysis

2.3.1 Spectral analysis

The co-spectrum between the cross-shore current velocity (u) and the suspended sediment concentration (ssc) at 0.05 m from the bed was calculated for each data set to determine the direction and magnitude of the cross-shore suspended sediment flux close to the bed (0.05 m) under different frequency components (swell waves, wind waves, and low frequency oscillations, such as wave groups and the group-bound long wave). Co-spectral analysis was conducted through digital Fourier transforms, with each data set of 4096 points divided into eight equal segments for the segment average method (Bendat and Piersol, 1986). The number of degrees of freedom used was 16. Estimates of the 95 % confidence interval indicated that the lower values of these spectra were 0.55 times the spectral estimates, and the upper values were 2.31 times the spectral estimates.

2.3.2 Net suspended sediment flux

The cross-shore suspended sediment flux at low frequencies was offshore at most sites, possibly due to the combined action of wave groups and the group-bound long wave (Shi and Larsen, 1984). In the swell frequency band, however, the suspended sediment flux direction varied over the different ripple types; thus the main focus of this study was swell waves.

For all the data sets, the u autospectrum showed most of the incident swell wave energy was between about 0.05 and 0.11 Hz (i.e. between 9 and 20 s). The area under the co-spectrum in this frequency band was integrated to yield the net cross-shore sediment flux due to swell waves. The net sediment flux values were then normalised by the absolute value of the area under the co-spectrum in the same frequency band to obtain the normalised net cross-shore sediment flux.

ESURFD

2, 215–254, 2014

The effect of ripple types on cross-shore

S. R. Kularatne et al.

Title Page

Abstract

Introduction

Conclusions

References

Tables

Figures

◀

▶

◀

▶

Back

Close

Full Screen / Esc

Printer-friendly Version

Interactive Discussion



2.4 Ripple classification

The ripples were classified according to their geometry and sediment resuspension patterns into five categories: post-vortex ripples, 2-D ripples, 2-D/3-D ripples, 3-D ripples, and cross ripples.

5 Low amplitude ripples oriented parallel to the wave crests were classified as post-vortex ripples when the ripple steepness was less than 0.1 (Osborne and Vincent, 1993). These ripples were sometimes absent because they were washed away during larger waves of the wave groups and re-formed during smaller waves. Vortex shedding occurred at irregular intervals, and diffusive mixing was the main cause of the sediment
10 resuspension that occurred.

Steep ripples oriented parallel to the wave crests were termed 2-D ripples. Clear vortex shedding was observed over these ripples. Ripples with small heights and variable lengths and no distinct parallel, linear crests were classed as 3-D ripples. The distance between bifurcations was smaller (< 10 cm) over 3-D ripples than it was over
15 2-D ripples, and sediment suspension also occurred as discrete packages. Ripples with geometries between the 2-D and 3-D classifications were called 2-D/3-D ripples. The bifurcation density for 2-D/3-D ripples was greater than it was for 2-D ripples, but less than it was for 3-D ripples. The heights of the 2-D/3-D ripples were greater than those of the 3-D ripples. The sediment suspension process over the 2-D/3-D ripples
20 resembled that of the 2-D ripples.

The last ripple type – cross ripples – consisted of large primary ripples and small secondary ripples, which were orthogonal to each other. Independently, each set of ripples could be considered 2-D. Although these ripples were 3-D in planform, they were classed separately from the 3-D ripples defined above because they were composed of distinct sets of parallel ripples, unlike the irregular nature of the 3-D ripples.
25 The primary and secondary ripples were inclined to the wave propagation direction by about $\pm 45^\circ$. Cross ripples can be considered vortex under Osborne and Vincent's (1993) classification.

ESURFD

2, 215–254, 2014

The effect of ripple types on cross-shore

S. R. Kularatne et al.

Title Page

Abstract

Introduction

Conclusions

References

Tables

Figures

◀

▶

◀

▶

Back

Close

Full Screen / Esc

Printer-friendly Version

Interactive Discussion



3 Results and discussion

Field measurements were collected at several low energy, microtidal beaches in south-western Australia to study the sediment resuspension and cross-shore suspended sediment transport over six ripple types (flat bed, post-vortex ripples, 2-D ripples, 2-D/3-D ripples, 3-D ripples, and cross ripples).

3.1 Ripple geometry

The mean ripple height and steepness values for the different ripple types are plotted in Fig. 2. Cross ripples had the highest mean ripple height (about 5 cm) because of their large primary ripples. The 2-D ripples had the second highest height, followed by the 2-D/3-D, 3-D, and post-vortex ripples (Fig. 2a). The post-vortex ripple heights were small with a mean value of ~ 0.6 cm.

The 2-D/3-D and 3-D ripples had greater ripple steepness values than the other ripple types because of their shorter lengths (Fig. 2b). The 2-D and cross ripples were gentler, as their lengths were greater. The mean ripple steepness for all the ripples types was greater than 0.1, except for the post-vortex ripples, which had the smallest mean steepness value of about 0.08.

3.2 Ripple patterns

The ripple type present can depend on the mobility number (ψ) and the grain size (represented by the median grain diameter, d_{50}) (Lofquist, 1978; O'Donoghue and Clubb, 2001; O'Donoghue et al., 2006). The mobility number here was calculated with $u_{1/10}$, for comparison with O'Donoghue et al. (2006), and is given by

$$\psi_{1/10} = \frac{u_{1/10}^2}{(s-1)gd_{50}} \quad (1)$$

ESURFD

2, 215–254, 2014

The effect of ripple types on cross-shore

S. R. Kularatne et al.

Title Page

Abstract

Introduction

Conclusions

References

Tables

Figures

◀

▶

◀

▶

Back

Close

Full Screen / Esc

Printer-friendly Version

Interactive Discussion



Where, $u_{1/10}$ is the mean of the highest one-tenth of the cross-shore velocity, s is the specific sediment gravity (2.65 for quartz sand), g is the gravitational acceleration, and d_{50} is the median grain diameter.

Flatbed conditions were observed under the highest mobility numbers ($\Psi_{1/10} > 100$), which corresponded to high bed shear stresses (Fig. 3); however, O'Donoghue et al. (2006) carried out several full-scale laboratory studies and found flatbed conditions occurred only when the $\Psi_{1/10}$ was > 190 . In this study, flat bed conditions occurred under breaking waves, or at least where the largest waves were breaking. The increased turbulence under these breaking conditions might have led to the formation of flat beds under lower mobility numbers; this might have also been the case for post-vortex ripples, which were observed under mobility numbers as low as ~ 50 . The field results revealed a large, single, random, breaking wave could flatten the developing vortex ripples maintaining the post-vortex bed.

Cross, 2-D, 2-D/3-D, and 3-D ripples were observed under similar mobility numbers ($\Psi_{1/10} \lesssim 80$). O'Donoghue et al. (2006) found the mobility number could not separate 2-D and 3-D ripples. The field results showed the grain size was better able to separate the 2-D and 3-D ripples. Two-dimensional ripples occurred when the D_{50} was $\gtrsim 0.35$ mm, and other ripple types occurred when the D_{50} was $\lesssim 0.35$ mm, as shown in Doucette (2000) and here in Fig. 3. Several full-scale laboratory studies (Lofquist, 1978; O'Donoghue and Clubb, 2001; O'Donoghue et al., 2006) have shown that grain size is the most important factor for differentiating between 2-D and 3-D ripples.

3.3 Suspended sediment concentration

The mean value of the highest one-third of the suspended sediment concentration (ssc_{sig}) at 0.05 m above the seabed was plotted against the ripple steepness (Fig. 4). Strong sediment resuspension was always present over steep ripples ($\eta/\lambda > 0.15$). This finding supports the hypothesis that steeper ripples induce more suspension (suspension enhanced by sand-laden separation vortices on the leeside of ripples) (Vincent et al., 1991; Osborne and Greenwood, 1993; Osborne and Vincent, 1996). Sediment

The effect of ripple types on cross-shore

S. R. Kularatne et al.

Title Page

Abstract

Introduction

Conclusions

References

Tables

Figures

◀

▶

◀

▶

Back

Close

Full Screen / Esc

Printer-friendly Version

Interactive Discussion



suspension was stronger over steep ripples than it was over gentle ripples and more diffusive over gentle ripples (Osborne and Vincent, 1996). The ripple geometry affected the sediment suspension pattern over the ripples, which might have affected the phase relationship between the u and the ssc and changed the direction of the suspended sediment flux.

3.4 Sediment suspension and wave groups

Simultaneous time series records of the u and the ssc over a flat bed at Leighton Beach are shown in Fig. 5a and b. The instrument station was deployed just outside the breaker line in a mean water depth (h) of 0.52 m, where the significant wave height to water depth ratio (H_s/h) was high (0.94).

The envelope function calculated using List's (1991) method (Fig. 5a) showed wave groups were present and high suspension events coincided with the passing of wave groups (Fig. 5b). Other studies have shown the presence of wave groups causes high suspension, and several explanations have been proposed: (1) Vincent et al. (1991) proposed that alternate changes in the ripple geometry during the passing of large and small waves of wave groups could cause high suspension when large waves met with steep ripples; (2) Villard and Osborne (2002) suggested antecedent waves could lead to coupling between antecedent and developing vortices above a rippled bed and hence cause high suspension. However, as shown in Fig. 5, high suspension due to wave groups has also been observed over flat beds; (3) over a flat bed, the larger waves of a wave group could produce persistent turbulence, which could cause high suspension as wave groups pass (Hanes and Huntley, 1986; Osborne and Greenwood, 1993; Kularatne and Pattiaratchi, 2008); (4) Hay and Bowen (1994a) suggested high suspension observed at the wave group frequency might have been the result of more than one action. They suggested vortex-shedding from megaripples, enhanced interaction with the seabed during larger waves of the wave groups (perhaps via the group-bound long wave), and coherent structures in the combined flow turbulence as possible causes; (5) Hay and Bowen (1994b) proposed bed forms, surface-injected vortices, and the

The effect of ripple types on cross-shore

S. R. Kularatne et al.

Title Page

Abstract

Introduction

Conclusions

References

Tables

Figures



Back

Close

Full Screen / Esc

Printer-friendly Version

Interactive Discussion



The effect of ripple types on cross-shore

S. R. Kularatne et al.

Title Page

Abstract

Introduction

Conclusions

References

Tables

Figures

◀

▶

◀

▶

Back

Close

Full Screen / Esc

Printer-friendly Version

Interactive Discussion



sensor support structure as possible causes for the pumping of sediments observed at the wave group frequency. They suggested that keeping the sensors 5–10 diameters from the nearest support would minimise the supporting structure's influence (Hay and Bowen, 1994a), as was the case in this study. High suspension was observed under wave groups over flat and rippled beds in this study.

3.5 Cross-shore suspended sediment flux

The cross-spectral and cross-correlation analyses between the time series records of the u and the c were used to study the variation in the direction and magnitude of the cross-shore suspended sediment flux over six ripple types (flat bed, post-vortex ripples, 2-D ripples, 2-D/3-D ripples, 3-D ripples, and cross ripples). Note that the ssc was measured only 0.05 m from the seabed; hence the sediment flux discussed here refers to sediment flux at that elevation. The mean values of the normalised net cross-shore suspended sediment flux in the swell frequency band calculated for the different ripple types are shown in Fig. 6. Onshore flux was defined as positive and offshore flux was defined as negative.

In the following descriptions of sediment flux over the different ripples types, the results from one model run are used for each ripple type.

3.5.1 Flatbed

Over a flat bed, the net sediment flux due to swell waves was mainly onshore (Fig. 6), which corresponded with the findings of Huntley and Hanes (1987), Osborne and Greenwood (1992b), and Davidson et al. (1993).

The spectral analysis results for the u and c (Fig. 5) are shown in Fig. 7, which also shows the instrument station location at Leighton Beach (Fig. 7a). The results showed the seabed was flat. The u autospectrum showed a main peak at around 0.075 Hz (~ 13 s), which corresponded to the incoming swell waves (Fig. 7b). The ssc autospectrum showed two peaks corresponding to wave groups and swell waves, with the highest

peak occurring in the wave group frequency band (< 0.025 Hz) (Fig. 7c). Conditions were swell-dominated, and the ssc spectrum showed wave groups suspended more sediments.

The co-spectrum between the u and the ssc (Fig. 7d) revealed the usual trend observed over a flatbed: the suspended sediment flux in the swell frequency band was onshore (the dotted lines show the frequency range chosen as the swell frequency band) and the flux at low frequencies was offshore (Huntley and Hanes, 1987). A smaller onshore component was observed at the first harmonic of the swell waves. The cross-spectrum (Fig. 7e) depicts the gross transport rates (addition of onshore and offshore transport) in the frequency domain. Swell waves were the main transport component.

The phase lag between the u and the ssc (Fig. 7f) indicated the sediment flux direction. Flux is onshore if the phase lag is less than $\pm 90^\circ$ because the peak in sediment concentration occurs while the cross-shore current velocity is onshore. Flux is offshore if the phase lag is more than $\pm 90^\circ$ because the sediment concentration peaks during the offshore phase. At this location, the phase lag was less than 90° in the swell frequency and first harmonic bands, resulting in onshore flux, and more than 90° out of phase at low frequencies, resulting in offshore flux.

The coherence spectrum (Jenkins and Watts, 1968) was used to calculate the 95% confidence interval for the phase spectrum (Davidson et al., 1993) for the main frequency components and to test the statistical significance of the main sediment flux components (Fig. 7f). The results showed the co-spectral peaks observed in the three main frequency bands (low frequencies, swell frequency band, and the first harmonic of the swell band) were statistically significant (Fig. 7e). Strong coherence peaks were observed between the u and the ssc in the swell frequency band and the first harmonic of the swell band; however, the coherence at low frequencies was low (Fig. 7g). This finding explained the stronger suspended sediment flux observed under swell waves than that observed under low frequency waves (Fig. 7d). Similar results were always obtained when the seabed was flat.

The effect of ripple types on cross-shore

S. R. Kularatne et al.

Title Page

Abstract

Introduction

Conclusions

References

Tables

Figures



Back

Close

Full Screen / Esc

Printer-friendly Version

Interactive Discussion



The effect of ripple types on cross-shore

S. R. Kularatne et al.

Title Page

Abstract

Introduction

Conclusions

References

Tables

Figures

◀

▶

◀

▶

Back

Close

Full Screen / Esc

Printer-friendly Version

Interactive Discussion



The increasing velocity skewness as waves shoaled was assumed to force the strong onshore sediment flux in the swell frequency band (Doering and Bowen, 1989; Osborne and Greenwood, 1992b). Flat beds were generally observed close to the shore (or on a bar's seaward slope), where the wave and velocity skewness were greatest.

Several studies have found that large fluid accelerations, skewed towards shore, suspend more sediment under near-breaking and breaking waves (Hanes and Huntley, 1986; Nielsen, 1992; Osborne and Greenwood, 1993) coinciding with the cross-shore velocity's onshore phase, resulting in onshore sediment transport (Elgar et al., 1988, 2001).

3.5.2 Post-vortex ripples

The net cross-shore sediment flux due to swell waves over post-vortex ripples was mainly offshore (Fig. 6). The u and ssc spectral analysis results for run 3 at Leighton Beach (Fig. 8a), where the seabed was covered with post-vortex ripples, are shown in Fig. 8c–h. This data set was collected at the same site as the data set shown in Fig. 7 (Leighton Beach), except that it was collected farther offshore (Fig. 8a). These results are representative of all the post-vortex ripple observations.

The u and ssc autospectra (Fig. 8c and d) showed the same trend as that shown in Fig. 7b and c, with the u peaking in the swell frequency band and the ssc peaking in the low frequency band. The co-spectrum between the u and the ssc (Fig. 8e) deviated from what was observed over a flat bed at this beach (Fig. 7d), with sediment flux in the swell frequency band moving offshore while the flux in the low frequency band remained offshore and the first harmonic of the swell band remained onshore. Inman and Bowen's (1963) description for offshore sediment flux observed over steep vortex ripples could not explain this result, as the ripples were post-vortex (steepness < 0.1), with no regular vortex formation observed. Offshore sediment flux over flat or post-vortex ripples has been observed in other studies (Osborne and Greenwood, 1992b; Brander and Greenwood, 1993; Masselink and Pattiaratchi, 2000). Davidson et al. (1993) also

noted offshore sediment flux when ripples were present, but as the ripple parameters were not measured, it was unclear whether the ripples were vortex or post-vortex.

The cross-correlation between the u and the ssc was calculated to examine the offshore flux observed in the swell frequency band. The cross-correlation coefficient revealed a dominant, negative peak with a lag of about 2 s, which suggested the peak in the ssc occurred 2 s after the wave trough had passed (Fig. 8b). Given that the peak period of the swell waves was ~ 14 s, this result showed the maximum ssc coincided with the wave motion's offshore phase, resulting in offshore flux.

Diffusive mixing has been identified as the main cause of sediment suspension over post-vortex ripples when no vortex forms (Osborne and Vincent, 1996; Masselink and Pattiaratchi, 2000). Osborne and Vincent (1996) found flow turbulence caused high sediment concentrations close to the bed over gentle ripples during the strong onshore phase, and that diffusion moved these sediments 2–5 cm up the water column during the offshore phase. The cross-correlation analysis (Fig. 8b), which showed a peak in the ssc at 0.05 m from the bed during the offshore phase, supported this finding.

The suspended sediment flux close to the bed due to swell waves over post-vortex ripples is shown in Fig. 9. During the strong onshore phase, the flow-induced turbulence increased the sediment concentration close to the bed (Fig. 9a). These sediments moved 2–5 cm up the water column during the offshore phase (Fig. 9b), which produced the net offshore sediment flux in the swell frequency band close to the bed (Fig. 9c).

3.5.3 2-D ripples

The net cross-shore suspended sediment flux due to swell waves over 2-D ripples was onshore (Fig. 6). The seabed at the four measurement sites at South Beach (Fig. 10a) was covered with 2-D ripples. The results of the spectral analysis between the u and the c for the site closest to the shore (Fig. 10a) are shown in Fig. 10c–h. The instrument station was deployed just outside the breaker line, where the mean water depth was 0.72 m.

The effect of ripple types on cross-shore

S. R. Kularatne et al.

Title Page

Abstract

Introduction

Conclusions

References

Tables

Figures

◀

▶

◀

▶

Back

Close

Full Screen / Esc

Printer-friendly Version

Interactive Discussion



The effect of ripple types on cross-shore

 S. R. Kularatne et al.

[Title Page](#)
[Abstract](#)
[Introduction](#)
[Conclusions](#)
[References](#)
[Tables](#)
[Figures](#)
[◀](#)
[▶](#)
[◀](#)
[▶](#)
[Back](#)
[Close](#)
[Full Screen / Esc](#)
[Printer-friendly Version](#)
[Interactive Discussion](#)


The u and ssc autospectra showed the same pattern that was observed throughout the study: swell waves dominated the u spectrum (Fig. 10c) and low frequency oscillations dominated the ssc spectrum (Fig. 10d). The co-spectrum between the u and the ssc showed onshore flux in the swell frequency band and negligible flux at low frequencies and in the first harmonic of the swell band (Fig. 10e). Clear vortex formation was observed over the 2-D ripples. These results disagreed with Inman and Bowen's (1963) theory that suspended sediment flux over vortex ripples was offshore; however, Osborne and Greenwood (1992b) and Brander and Greenwood (1993) also measured onshore flux over steep ripples.

The cross-correlation coefficient between the u and the ssc showed a positive peak with a time lag of about 1 s, which suggested the maximum ssc appeared 1 s after the onshore velocity maxima occurred (Fig. 10b). This result suggested the leeside vortices were ejected just after the maxima in the cross-shore velocity occurred while the flow was still directed onshore. A possible explanation for the onshore suspended sediment flux observed over 2-D (vortex) ripples is depicted in Fig. 11. Here leeside separation vortices formed during the strong onshore phase (Fig. 11a). These sand-laden vortices were ejected into the flow while the flow was still onshore (Fig. 11b), which caused onshore sediment flux at the sensor location (Fig. 11c). This sediment might have then quickly settled below the sensor on flow reversal.

3.5.4 2-D/3-D ripples

The net suspended sediment flux due to swell waves over 2-D/3-D ripples was mainly onshore (Fig. 6). The spectral analysis results obtained from a data set collected at south Pinnaroo Beach are shown in Fig. 12.

The instrument station was 25 m offshore in a water depth of 1.17 m (Fig. 12a). Similar to most of the data sets that were examined, the u spectrum peaked in the swell frequency band (Fig. 12b), and the ssc spectrum peaked at low frequencies (Fig. 12c). The co-spectrum between the u and the ssc showed a similar trend to that observed over the 2-D ripples, with strong onshore flux in the swell frequency band and neg-

ligible offshore flux at low frequencies (Fig. 12d). Overall, the cross-spectral analysis results for the 2-D/3-D ripples resembled those of the 2-D ripples. In situ observations further suggested that 2-D/3-D ripples resembled 2-D ripples. Thus the explanation for 2-D ripples depicted in Fig. 11 could be applied to the mainly onshore sediment flux observed over 2-D/3-D ripples.

3.5.5 3-D ripples

The net cross-shore sediment flux close to the seabed due to swell waves over 3-D ripples was mainly offshore (Fig. 6). The u and ssc spectral analysis results for a site at Warnbro Sound (Fig. 13a), where the seabed was covered with 3-D ripples, are shown in Fig. 13c–h.

The instrument station was about 30 m from the shore in a mean water depth of 0.8 m. The significant wave height to water depth ratio (H_s/h) was 0.182. The u and ssc autospectra showed the same pattern observed throughout the study: swell waves dominated the u spectrum (Fig. 13c) and low frequency oscillations dominated the ssc spectrum (Fig. 13d). The co-spectrum between the u and the ssc showed a similar trend to that observed over the post-vortex ripples, with strong offshore sediment flux in the swell frequency band and weak offshore flux at low frequencies (Fig. 13e).

The cross-correlation between the time series of the u and the ssc is shown in Fig. 13b. A negative correlation with approximately zero lag was observed, which suggested the peak in the offshore velocity coincided with the peak in ssc. The sediment suspension pattern over the 3-D ripples, however, was different from that of the post-vortex ripples; therefore the same explanation was not applicable. Three-dimensional ripples can be classified as vortex under Clifton and Dinger's (1984) classification, and the sediment suspension occurred as discrete packages.

Three-dimensional ripples were always observed in deep water where the wave asymmetry was less. Details of the observed ripples (water depth, distance from shore, and H_s/h) at three sites are presented in Table 1 (with details of the 3-D ripples highlighted in bold). Three-dimensional ripples were seen when the H_s/h was low and the

The effect of ripple types on cross-shore

S. R. Kularatne et al.

Title Page

Abstract

Introduction

Conclusions

References

Tables

Figures

◀

▶

◀

▶

Back

Close

Full Screen / Esc

Printer-friendly Version

Interactive Discussion



Discussion Paper | Discussion Paper | Discussion Paper | Discussion Paper | Discussion Paper

The effect of ripple types on cross-shore

S. R. Kularatne et al.

Title Page

Abstract

Introduction

Conclusions

References

Tables

Figures

◀

▶

◀

▶

Back

Close

Full Screen / Esc

Printer-friendly Version

Interactive Discussion



shoaling waves were less asymmetric towards the shore. The H_s/h reduced with increasing cross-shore distance from the shore except when a bar was present. This decreased wave asymmetry might have caused the difference in the vortex ejection timing between the 2-D and 3-D ripples. The vortices might not have been ejected into the flow as quickly under weak peak onshore velocities, and the 3-D ripples' small heights might have also affected this difference in the vortex ejection timing.

3.5.6 Cross ripples

Although the mean cross shore sediment flux indicated a net onshore flux over cross ripples in the swell frequency band (Fig. 6), the large standard error revealed that both onshore and offshore net fluxes occurred. The co-spectra between the u and the ssc were calculated for cross ripples at six sites (Fig. 14). Onshore sediment flux in the swell frequency band can be seen in Fig. 14a, b, and f. Offshore flux can be seen in Fig. 14c–e, and reveals the variability in the direction of the suspended sediment flux.

The cross ripples consisted of large primary and small secondary ripples, which were orthogonal to each other and oblique to the wave propagation direction by about $\pm 45^\circ$ (Fig. 15). The cross ripples' geometry is shown in Table 2. At most sites, the ripple steepness was greater than 0.1 and hence could be considered vortex (Osborne and Vincent, 1993); however, no trend was found between the ripple parameters and the direction of the cross-shore sediment flux.

The combined effect of the large primary and small secondary ripples and the different positioning of the instruments relative to the primary and secondary ripples might have caused the variability in the direction of the cross-shore sediment flux.

4 Implications

The type of ripples present affects the sediment resuspension occurring above the ripples and the sediment resuspension's temporal and spatial relationship to the near-bed

The effect of ripple types on cross-shore

S. R. Kularatne et al.

Title Page

Abstract

Introduction

Conclusions

References

Tables

Figures

◀

▶

◀

▶

Back

Close

Full Screen / Esc

Printer-friendly Version

Interactive Discussion



oscillatory flow (Nielsen, 1992; Osborne and Vincent, 1993, 1996), which can change the direction of the suspended sediment flux due to incident swell waves over different ripple types (Osborne and Greenwood, 1992a; Brander and Greenwood, 1993; Davidson et al., 1993); however, few studies have examined the sediment resuspension and flux over different ripple types (Brander and Greenwood, 1993; Osborne and Vincent, 1993, 1996).

This study examined the cross-shore flux and sediment resuspension in the frequency domain in a low energy environment over six ripple types. The results showed that ripples changed the flow field and sediment suspension close to the seabed. The direction of the suspended sediment flux in the swell frequency band depended on the ripple type. The suspended sediment flux was consistently onshore over flat beds, 2-D ripples, and 2-D/3-D ripples, and offshore over 3-D and post-vortex ripples. Over cross ripples, the suspended sediment flux direction was variable. The direction of the cross-shore sediment flux over the different ripple types, and possible causes for the observed variation, is presented in Table 3.

5 Conclusions

The measurements obtained from low energy beaches in south-western Australia for different ripple types (flat bed, post-vortex ripples, 2-D ripples, 2-D/3-D ripples, 3-D ripples, and cross ripples) revealed the following:

- the mobility number ($\psi_{1/10}$), based on the highest one-tenth of orbital velocities, can be used to delineate between flat bed and post-vortex ripples. Flat bed conditions were observed when the $\psi_{1/10}$ was > 100 , and post-vortex ripples were present when $50 < \psi_{1/10} < 140$. No clear boundaries in the mobility number were observed among the other ripple types that occurred when the $\psi_{1/10}$ was $\lesssim 80$.
- Two-dimensional ripples were observed in the presence of coarse grains ($d_{50} > 0.35$ mm). All other ripple types were observed when the d_{50} was < 0.35 mm.

The effect of ripple types on cross-shore

S. R. Kularatne et al.

Title Page

Abstract

Introduction

Conclusions

References

Tables

Figures

◀

▶

◀

▶

Back

Close

Full Screen / Esc

Printer-friendly Version

Interactive Discussion



– High suspended sediment concentration values were observed when the ripple steepness (η/λ) was high (> 0.15), possibly due to the ejection of sand by the vortices formed in the leeside of the ripples. The suspended sediment concentration was low when the η/λ was < 0.15 .

– The net cross-shore suspended sediment flux close to the seabed (at ~ 0.05 m) in the swell frequency band varied depending on the ripple type present. The suspended sediment flux was consistently onshore over flat beds, 2-D ripples, and 2-D/3-D ripples, and offshore over post-vortex ripples and 3-D ripples. Over cross ripples, the sediment flux direction was variable.

Acknowledgements. We acknowledge the award of an International Postgraduate Research Scholarship and University Postgraduate Award (to S.K.) and Ruth Gongora-Mesas for her editorial suggestions on the manuscript. This paper is in memory of Samantha Kularatne who tragically passed away in September 2009.

References

Bailard, J. A. and Inman, D. L.: A re-examination of Bagnold's granular-fluid model and bedload transport equation, *J. Geophys. Res.*, 84, 7827–7833, 1979.

Bendat, J. S. and Piersol, A. G.: *Random Data: Analysis and Measurement Procedures*, Wiley-Interscience, New York, 1986.

Brander, R. W. and Greenwood, B.: Bedform roughness and the re-suspension and transport of sand under shoaling and breaking waves: a field study, *Proceedings of the Canadian Coastal Conference*, Vancouver, BC, 587–599, 1993.

Brenninkmeyer, B. M.: In situ measurements of rapidly fluctuating, high sediment concentrations, *Mar. Geol.*, 20, 117–128, 1976.

Clifton, H. E. and Dingler, J. R.: Wave-formed structures and paleoenvironmental reconstruction, *Mar. Geol.*, 60, 165–198, 1984.

Davidson, M. A., Russell, P. E., Huntley, D. A., and Hardisty, J.: Tidal asymmetry in suspended sand transport on a macrotidal intermediate beach, *Mar. Geol.*, 110, 333–353, 1993.

The effect of ripple types on cross-shore

 S. R. Kularatne et al.

[Title Page](#)
[Abstract](#)
[Introduction](#)
[Conclusions](#)
[References](#)
[Tables](#)
[Figures](#)
[◀](#)
[▶](#)
[◀](#)
[▶](#)
[Back](#)
[Close](#)
[Full Screen / Esc](#)
[Printer-friendly Version](#)
[Interactive Discussion](#)


- Doering, J. C. and Bowen, A. J.: Wave-induced flow and nearshore suspended sediment, in: Coastal Engineering (1988): Proceedings of the Twenty-first International Coastal Engineering Conference, edited by: Edge, B. L., American Society of Civil Engineers, New York, 1452–1463, 1989.
- 5 Doucette, J. S.: The distribution of nearshore bedforms and effects of sand suspension on low-energy, micro-tidal beaches in southwestern Australia, *Mar. Geol.*, 165, 41–61, 2000.
- Elgar, S., Guza, R. T., and Freilich, M. H.: Eulerian measurements of horizontal accelerations in shoaling gravity waves, *J. Geophys. Res.*, 93, 9261–9269, 1988.
- Elgar, S., Gallagher, E. L., and Guza, R. T.: Nearshore sandbar migration, *J. Geophys. Res.*, 106, 11623–11628, 2001.
- 10 Hanes, D. M.: Intermittent sediment suspension and its implications to sand tracer dispersal in wave-dominated environments, *Mar. Geol.*, 81, 175–183, 1988.
- Hanes, D. M. and Huntley, D. A.: Continuous measurements of suspended sand concentration in a wave dominated nearshore environment, *Cont. Shelf. Res.*, 6, 585–596, 1986.
- 15 Hanson, H., Larson, M., and Kraus, N. C.: Calculation of beach change under interacting cross-shore and longshore processes, *Coast. Eng.*, 57, 610–619, 2010.
- Hay, A. E. and Bowen, A. J.: Coherence scales of wave-induced suspended sand concentration fluctuations, *J. Geophys. Res.*, 99, 12749–12766, 1994a.
- Hay, A. E. and Bowen, A. J.: Space-time variability of sediment suspension in the nearshore zone, in: Coastal Dynamics '94: Proceedings of an International Conference on the Role of the Large Scale Experiments in Coastal Research, edited by: Arcilla, A. S., Stive, M. J. F., and Kraus, N. C., American Society of Civil Engineers, New York, 962–975, 1994b.
- 20 Huntley, D. A. and Hanes, D. M.: Direct measurement of suspended sediment transport, in: Coastal Sediments 1987: Proceedings of a Specialty Conference on Advances in Understanding of Coastal Sediment Processes, edited by: Kraus, N. C., American Society of Civil Engineers, New York, 723–737, 1987.
- 25 Hurther, D. and Thorne, P. D.: Suspension and near-bed load sediment transport processes above a migrating, sand-rippled bed under shoaling waves, *J. Geophys. Res.*, 116, C07001, doi:10.1029/2010JC006774, 2011.
- 30 Inman, D. L. and Bowen, A. J.: Flume experiments on sand transport by waves and currents, Proceedings of the Eighth International Coastal Engineering Conference, American Society of Civil Engineers, Mexico City, 137–150, 1963.

The effect of ripple types on cross-shore

S. R. Kularatne et al.

Title Page

Abstract

Introduction

Conclusions

References

Tables

Figures

◀

▶

◀

▶

Back

Close

Full Screen / Esc

Printer-friendly Version

Interactive Discussion



Jenkins, G. M. and Watts, D. G.: Spectral Analysis and its Applications, Holden-Day, San Francisco, 1968.

Kularatne, S. R. and Pattiaratchi, C. B.: Turbulent kinetic energy and sediment resuspension due to wave groups, *Cont. Shelf. Res.*, 28, 726–736, 2008.

5 Lee, T. H. and Hanes, D. M.: Comparison of field observations of the vertical distribution of suspended sand and its prediction by models, *J. Geophys. Res.*, 101, 3561–3572, 1996.

List, J. H.: Wave groupiness variations in the nearshore, *Coast. Eng.*, 15, 475–496, 1991.

Lofquist, K. E. B.: Sand ripple growth in an oscillatory-flow water tunnel, Technical paper no. 78-5, Coastal Engineering Research Centre, US Army Corps of Engineers, 1978.

10 Masselink, G. and Pattiaratchi, C. B.: Tidal asymmetry in sediment resuspension on a macrotidal beach in northwestern Australia, *Mar. Geol.*, 163, 257–274, 2000.

Masselink, G., Austin, M. J., O'Hare, T. J., and Russell, P. E.: Geometry and dynamics of wave ripples in the nearshore zone of a coarse sandy beach, *J. Geophys. Res.*, 112, C10022, doi:10.1029/2006JC003839, 2007.

15 Nielsen, P.: Some basic concepts of wave sediment transport, Series paper 20, Institute of Hydrodynamics and Hydraulic Engineering, Technical University of Denmark, Lyngby, 1979.

Nielsen, P.: Field measurements of time-averaged suspended sediment concentrations under waves, *Coast. Eng.*, 8, 51–72, 1984.

Nielsen, P.: Coastal Bottom Boundary Layers and Sediment Transport, *Advanced Series on Ocean Engineering*, vol. 4, World Scientific, Singapore, 1992.

20 O'Donoghue, T. and Clubb, G. S.: Sand ripples generated by regular oscillatory flow, *Coast. Eng.*, 44, 101–115, 2001.

O'Donoghue, T., Doucette, J. S., van der Werf, J. J., and Ribberink, J. S.: The dimensions of sand ripples in full-scale oscillatory flows, *Coast. Eng.*, 53, 997–1012, 2006.

25 Osborne, P. D. and Greenwood, B.: Frequency dependent cross-shore suspended sediment transport, 1. A non-barred shoreface, *Mar. Geol.*, 106, 1–24, 1992a.

Osborne, P. D. and Greenwood, B.: Frequency dependent cross-shore suspended sediment transport, 2. A barred shoreface, *Mar. Geol.*, 106, 25–51, 1992b.

Osborne, P. D. and Greenwood, B.: Sediment suspension under waves and currents: time scales and vertical structure, *Sedimentology*, 40, 599–622, 1993.

30 Osborne, P. D. and Vincent, C. E.: Dynamics of large and small scale bedforms on a macrotidal shoreface under shoaling and breaking waves, *Mar. Geol.*, 115, 207–226, 1993.

ESURFD

2, 215–254, 2014

The effect of ripple types on cross-shore

S. R. Kularatne et al.

Title Page

Abstract

Introduction

Conclusions

References

Tables

Figures

I◀

▶I

◀

▶

Back

Close

Full Screen / Esc

Printer-friendly Version

Interactive Discussion



- Osborne, P. D. and Vincent, C. E.: Vertical and horizontal structure in suspended sand concentrations and wave-induced fluxes over bedforms, *Mar. Geol.*, 131, 195–208, 1996.
- Shi, N. C. and Larsen, L. H.: Reverse sediment transport induced by amplitude-modulated waves, *Mar. Geol.*, 54, 181–200, 1984.
- 5 Sternberg, R. W., Shi, N. C., and Downing, J. P.: Continuous measurements of suspended sediment, in: *Nearshore Sediment Transport*, edited by: Seymour, R. J., Springer, New York, 231–257, 1989.
- Villard, P. V. and Osborne, P. D.: Visualization of wave-induced suspension patterns over two-dimensional bedforms, *Sedimentology*, 49, 363–378, 2002.
- 10 Vincent, C. E., Hanes, D. M., and Bowen, A. J.: Acoustic measurements of suspended sand on the shoreface and the control of concentration by bed roughness, *Mar. Geol.*, 96, 1–18, 1991.

The effect of ripple types on cross-shore

S. R. Kularatne et al.

Title Page

Abstract

Introduction

Conclusions

References

Tables

Figures

◀

▶

◀

▶

Back

Close

Full Screen / Esc

Printer-friendly Version

Interactive Discussion



Table 1. Details of the observed ripples (distance from shore, mean water depth, and significant wave height to water depth ratio, H_s/h) at Eagle Bay, Warnbro Sound, and Safety Bay.

Location	Ripple type	Distance from shore (m)	Water depth (m)	H_s/h
Eagle Bay	Flat bed	6	0.25	0.75
	Cross	9	0.54	0.36
	3-D	18	0.95	0.20
	Cross	30	0.82	0.24
	3-D	54	1.25	0.16
Warnbro Sound	Cross	8	0.46	0.29
	2-D	10	0.55	0.32
	Post-vortex	22	0.27	0.68
	Cross	25	0.51	0.35
	3-D	31	0.80	0.18
Safety Bay	Post-vortex	5	0.26	0.61
	Cross	7	0.43	0.41
	3-D	17	0.71	0.19
	3-D	25	0.60	0.29
	3-D	35	0.99	0.13

The effect of ripple types on cross-shore

S. R. Kularatne et al.

Title Page

Abstract

Introduction

Conclusions

References

Tables

Figures

◀

▶

◀

▶

Back

Close

Full Screen / Esc

Printer-friendly Version

Interactive Discussion



Table 2. Ripple heights, lengths, and steepness for the primary and secondary ripples of the cross ripples measured at the field sites.

Location	Primary ripples			Secondary ripples		
	Ripple height (cm)	Ripple length (cm)	Ripple steepness	Ripple height (cm)	Ripple length (cm)	Ripple steepness
Eagle Bay 2	11	57	0.19	4	15	0.27
Eagle Bay 4	8.5	50	0.17	4	15	0.27
Warnbro Sound 1	5.5	25	0.22	3.5	8	0.44
Warnbro Sound 4	8	26	0.31	3.5	13	0.27
Safety Bay 2	1.75	17.5	0.1	1.5	10	0.15
Port-2 2	5.5	45	0.12	3.5	8.5	0.41
North Boulanger point 3	4	17.5	0.23	2	8	0.25
Jurien Bay Jetty 1	4	35	0.11	1	15	0.07

The effect of ripple types on cross-shore

S. R. Kularatne et al.

Table 3. The direction of the suspended sediment flux in the swell frequency band for the different ripple types and possible causes for the observed variation.

Ripple type	Direction of sediment flux due to swell waves	Process
Flat bed	Onshore	Increased velocity skewness
Post-vortex ripples	Offshore	Asymmetry in diffusive suspension (see Fig. 8)
2-D ripples	Onshore	Timing of flow and vortex ejection (see Fig. 10)
2-D/3-D ripples	Onshore	Same as for 2-D ripples
3-D ripples	Offshore	Low wave asymmetry in the onshore direction
Cross ripples	Onshore/offshore	Combined effect of primary and secondary ripples and relative sensor positioning

Title Page

Abstract

Introduction

Conclusions

References

Tables

Figures

◀

▶

◀

▶

Back

Close

Full Screen / Esc

Printer-friendly Version

Interactive Discussion



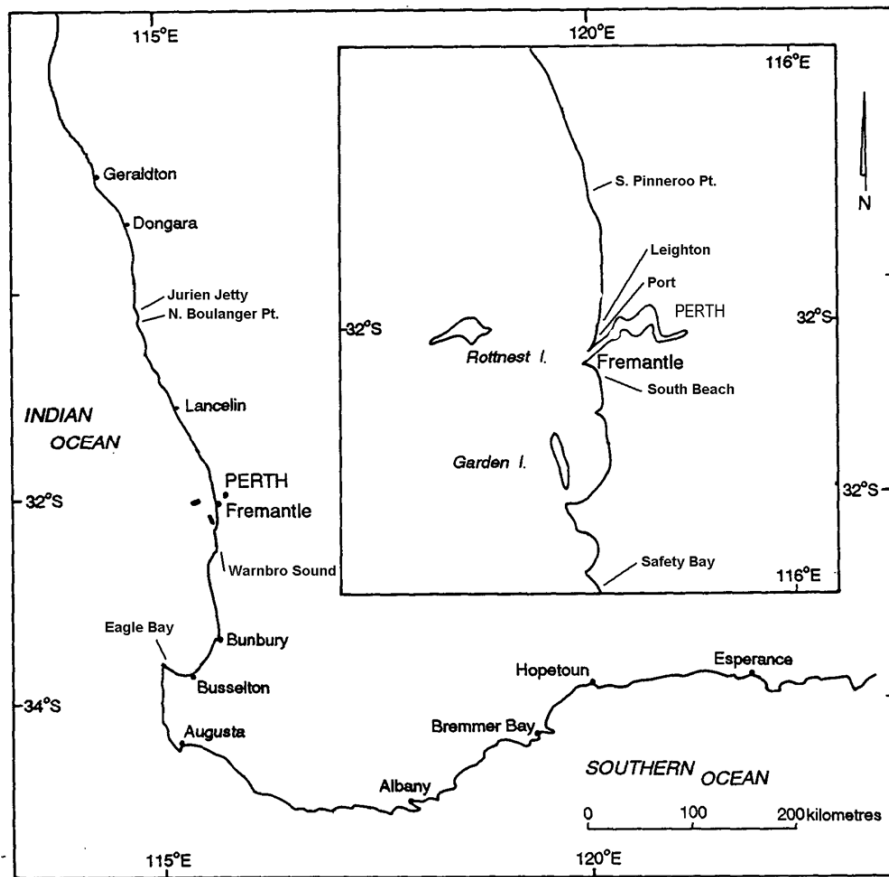


Fig. 1. Locations of the study sites.

The effect of ripple types on cross-shore

S. R. Kularatne et al.

Title Page	
Abstract	Introduction
Conclusions	References
Tables	Figures
◀	▶
◀	▶
Back	Close
Full Screen / Esc	
Printer-friendly Version	
Interactive Discussion	



The effect of ripple types on cross-shore

S. R. Kularatne et al.

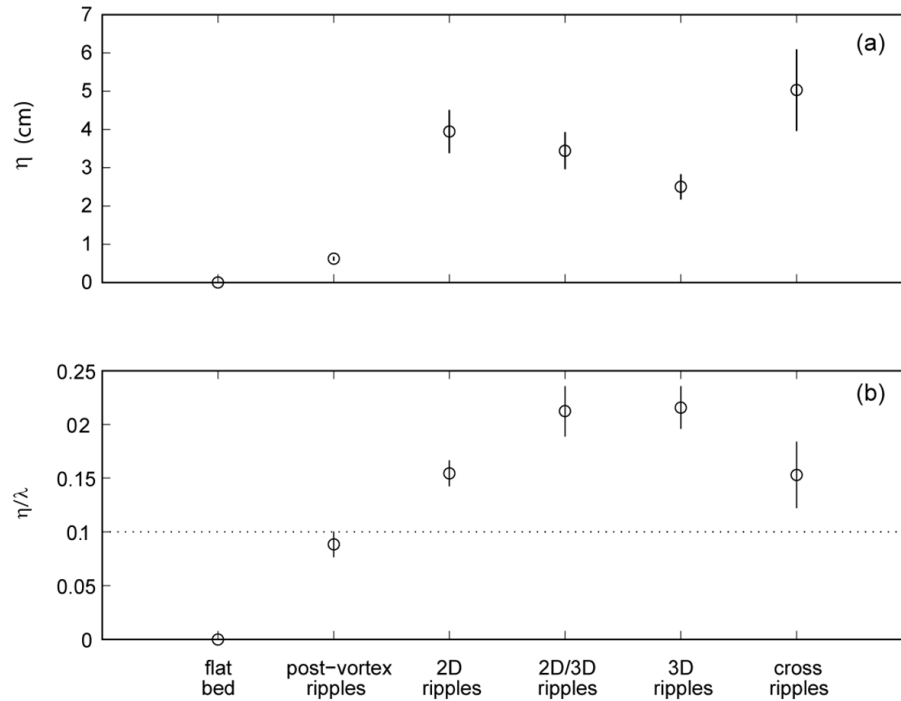


Fig. 2. (a) Average ripple height and (b) average ripple steepness for the different ripple types. Error bars denote the standard error around the average values.

Title Page

Abstract

Introduction

Conclusions

References

Tables

Figures

◀

▶

◀

▶

Back

Close

Full Screen / Esc

Printer-friendly Version

Interactive Discussion



The effect of ripple types on cross-shore

S. R. Kularatne et al.

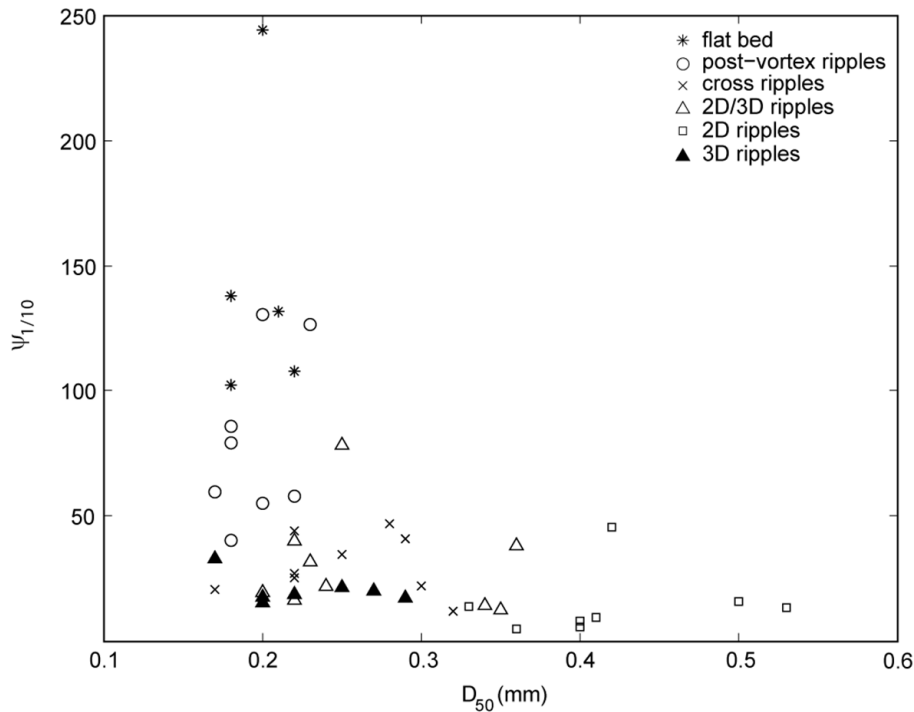


Fig. 3. Change in ripple type with the mobility number ($\Psi_{1/10}$) and median sand grain diameter (d_{50}).

Title Page

Abstract Introduction

Conclusions References

Tables Figures

◀ ▶

◀ ▶

Back Close

Full Screen / Esc

Printer-friendly Version

Interactive Discussion



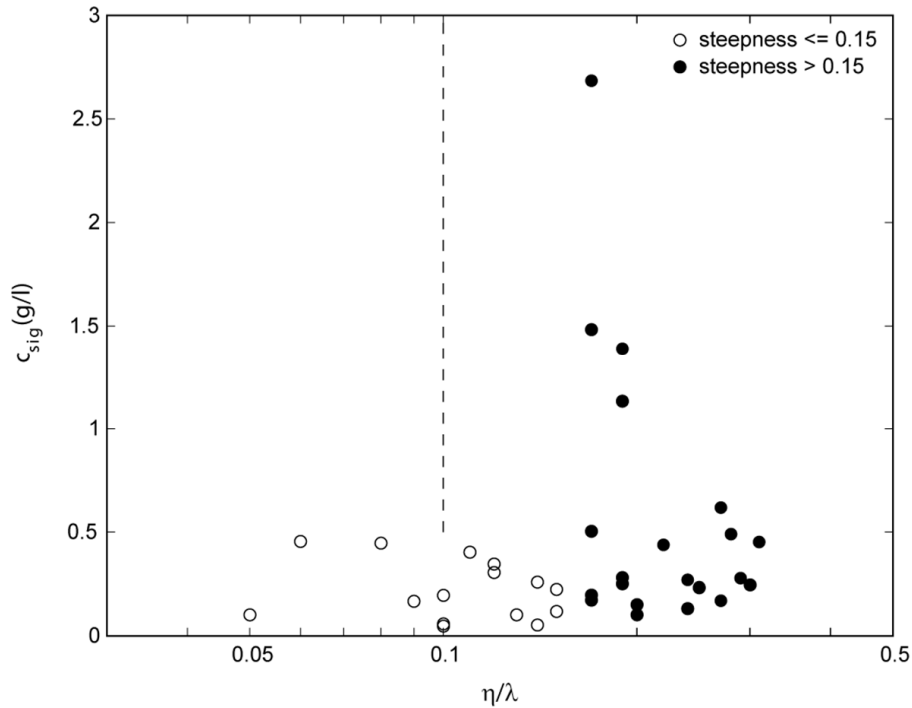


Fig. 4. Variation of the suspended sediment concentration with the ripple steepness (η/λ).

The effect of ripple types on cross-shore

S. R. Kularatne et al.

Title Page

Abstract Introduction

Conclusions References

Tables Figures

◀ ▶

◀ ▶

Back Close

Full Screen / Esc

Printer-friendly Version

Interactive Discussion



The effect of ripple types on cross-shore

S. R. Kularatne et al.

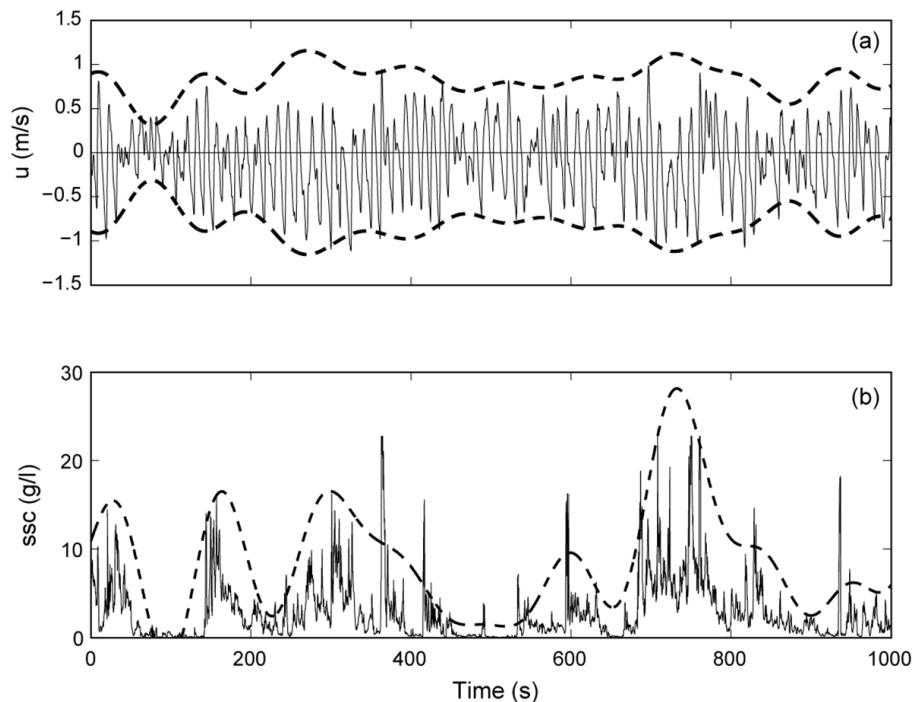


Fig. 5. Time series of the **(a)** cross-shore current velocity (u) ($z = 0.25$ m; solid line) and envelope function of the u (thick, dashed line) and **(b)** suspended sediment concentration ($c_{0.05}$) ($z = 0.05$ m; solid line) and low-pass-filtered $c_{0.05}$ (thick, dashed line). Data obtained from Leighton Beach.

Title Page

Abstract

Introduction

Conclusions

References

Tables

Figures

◀

▶

◀

▶

Back

Close

Full Screen / Esc

Printer-friendly Version

Interactive Discussion



The effect of ripple types on cross-shore

S. R. Kularatne et al.

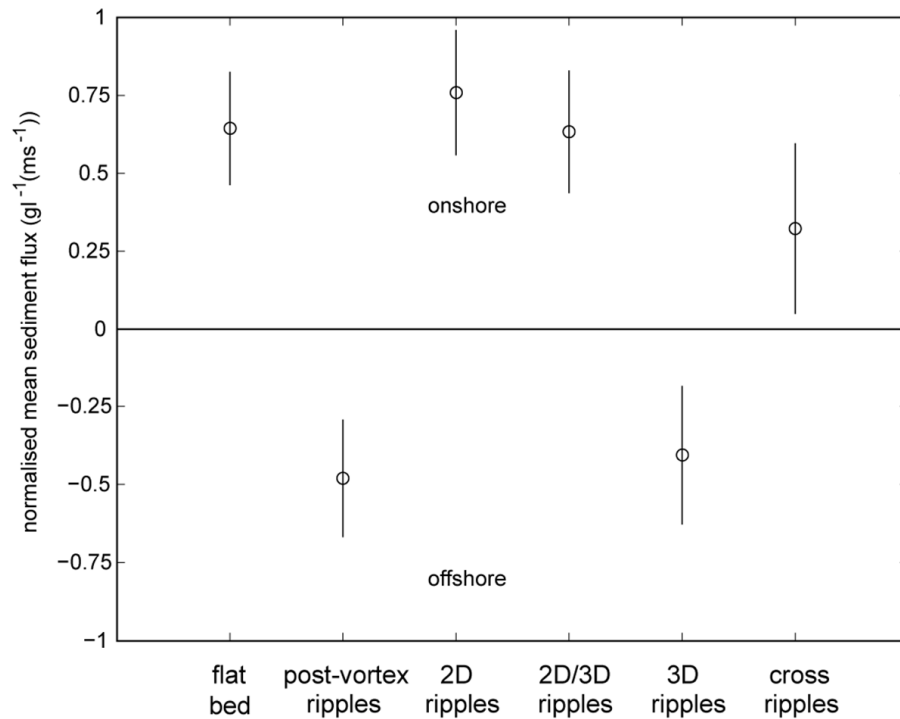


Fig. 6. Normalised net sediment flux over the different ripple types.

Title Page

Abstract

Introduction

Conclusions

References

Tables

Figures

◀

▶

◀

▶

Back

Close

Full Screen / Esc

Printer-friendly Version

Interactive Discussion



The effect of ripple types on cross-shore

S. R. Kularatne et al.

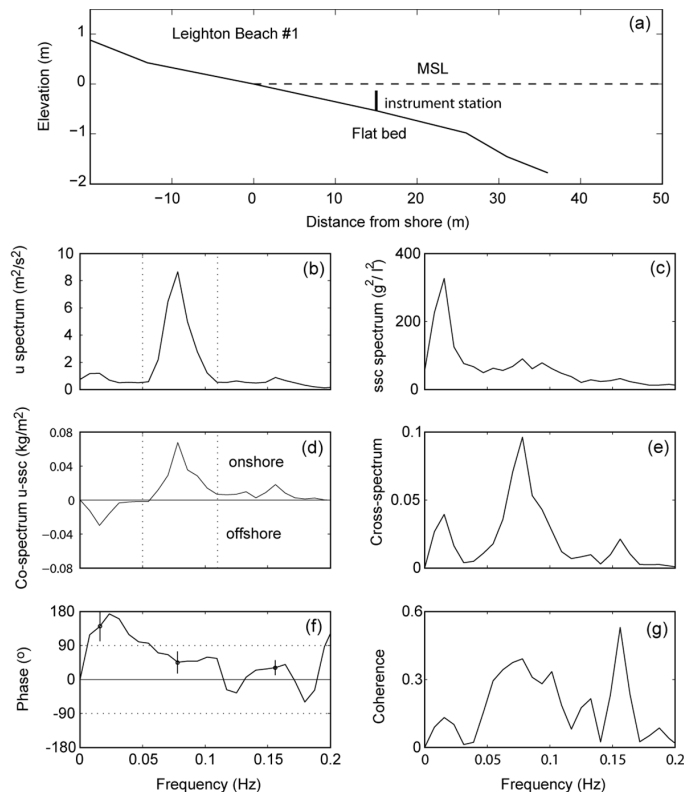


Fig. 7. (a) Beach profile for run 1 at Leighton Beach (over a flatbed). Results of the cross-spectral analysis between the cross-shore current velocity (u) and suspended sediment concentration ($c_{0.05}$) for run 1 at Leighton Beach (over a flatbed): (b) u autospectrum; (c) ssc autospectrum; (d) u -ssc co-spectrum; (e) u -ssc cross-spectrum; (f) u -ssc phase spectrum; (g) u -ssc coherence spectrum.

The effect of ripple types on cross-shore

S. R. Kularatne et al.

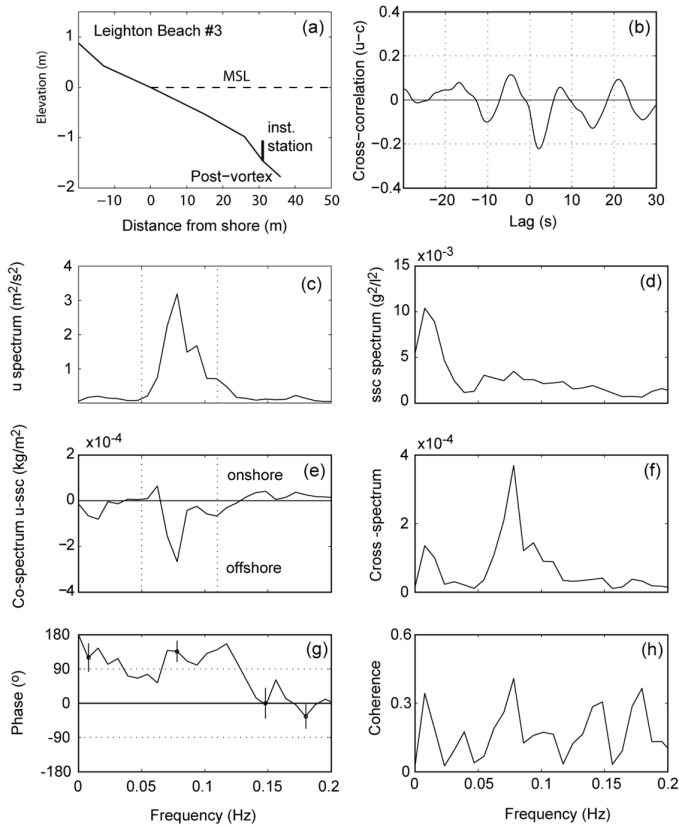


Fig. 8. (a) Beach profile for run 3 at Leighton Beach (over post-vortex ripples). Results of the cross-spectral analysis between the cross-shore current velocity (u) and suspended sediment concentration ($c_{0.05}$) for run 3 at Leighton Beach (over post-vortex ripples): (b) cross-correlation between u and $c_{0.05}$; (c) u autospectrum; (d) ssc autospectrum; (e) u -ssc co-spectrum; (f) u -ssc cross-spectrum; (g) u -ssc phase spectrum; (h) u -ssc coherence spectrum.

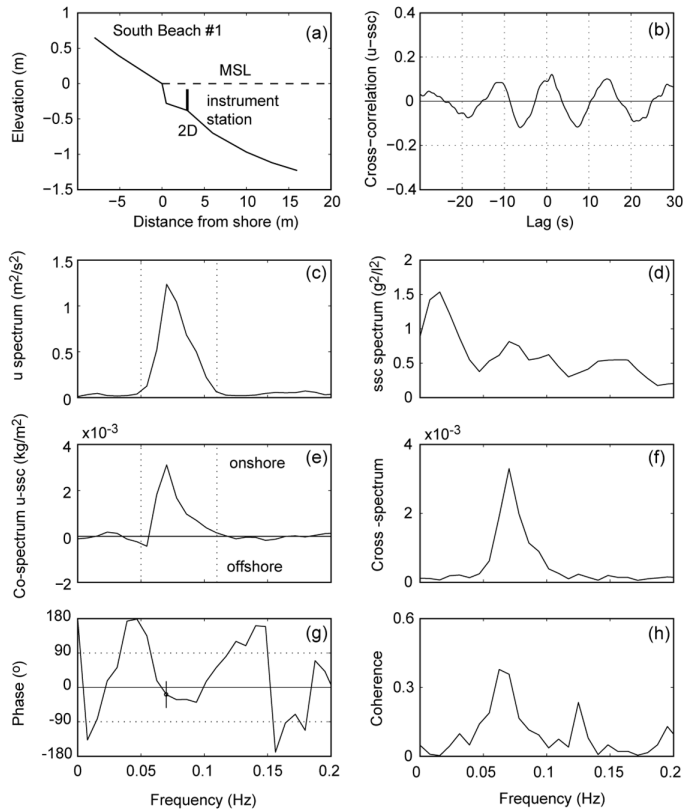


Fig. 10. (a) Beach profile for run 1 at South Beach (over 2-D ripples). Results of the cross-spectral analysis between the cross-shore current velocity (u) and suspended sediment concentration ($c_{0.05}$) for run 1 at South Beach (over 2-D ripples): (b) cross-correlation between u and $c_{0.05}$; (c) u autospectrum; (d) ssc autospectrum; (e) u -ssc co-spectrum; (f) u -ssc cross-spectrum; (g) u -ssc phase spectrum; (h) u -ssc coherence spectrum.

Title Page

Abstract Introduction

Conclusions References

Tables Figures

◀ ▶

◀ ▶

Back Close

Full Screen / Esc

Printer-friendly Version

Interactive Discussion



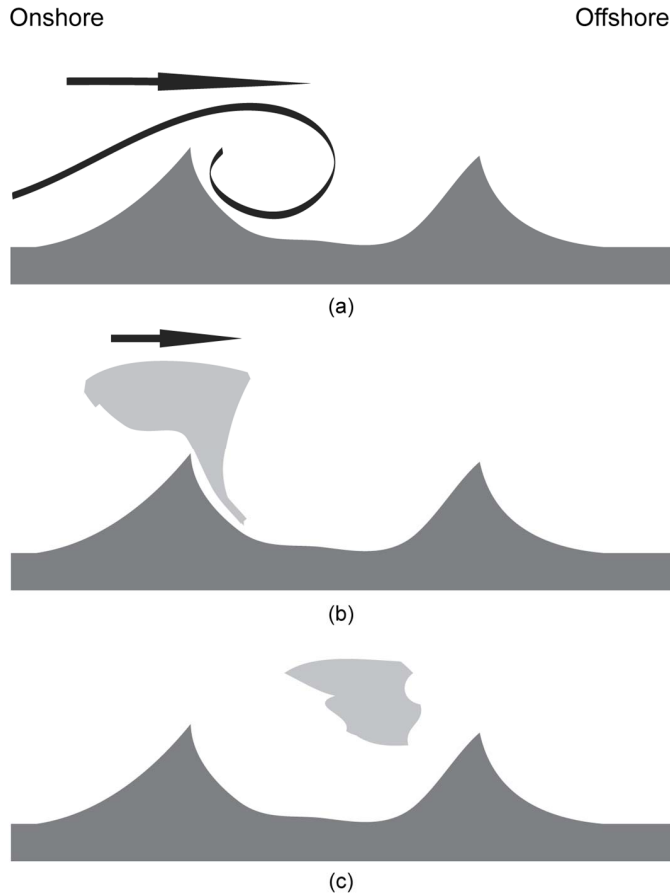


Fig. 11. Simple mechanism for onshore suspended sediment transport over vortex ripples (see text for explanation).

The effect of ripple types on cross-shore

S. R. Kularatne et al.

Title Page	
Abstract	Introduction
Conclusions	References
Tables	Figures
◀	▶
◀	▶
Back	Close
Full Screen / Esc	
Printer-friendly Version	
Interactive Discussion	



The effect of ripple types on cross-shore

S. R. Kularatne et al.

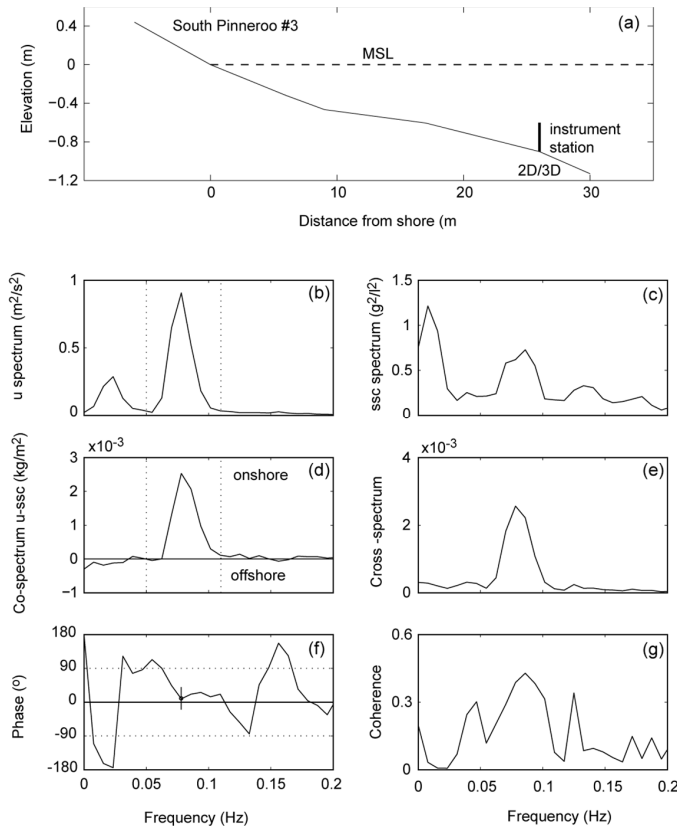


Fig. 12. (a) Beach profile for run 3 at south Pinnaroo (over 2-D/3-D ripples). Results of the cross-spectral analysis between the cross-shore current velocity (u) and suspended sediment concentration ($c_{0.05}$) for run 3 at south Pinnaroo (over 2-D/3-D ripples): (b) u autospectrum; (c) ssc autospectrum; (d) u -ssc co-spectrum; (e) u -ssc cross-spectrum; (f) u -ssc phase spectrum; (g) u -ssc coherence spectrum.



Title Page

Abstract Introduction

Conclusions References

Tables Figures

◀ ▶

◀ ▶

Back Close

Full Screen / Esc

Printer-friendly Version

Interactive Discussion

The effect of ripple types on cross-shore

S. R. Kularatne et al.

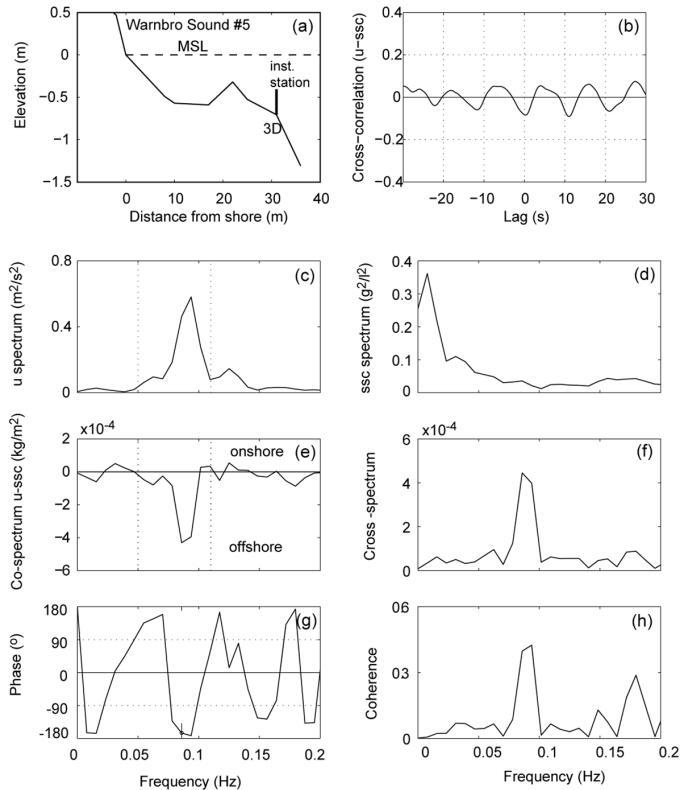


Fig. 13. (a) Beach profile for run 5 at Warnbro Sound (over 3-D ripples). Results of the cross-spectral analysis between the cross-shore current velocity (u) and suspended sediment concentration ($c_{0.05}$) for run 5 at Warnbro Sound (over 3-D ripples): (b) cross-correlation between u and $c_{0.05}$; (c) u autospectrum; (d) ssc autospectrum; (e) u -ssc co-spectrum; (f) u -ssc cross-spectrum; (g) u -ssc phase spectrum; (h) u -ssc coherence spectrum.

The effect of ripple types on cross-shore

S. R. Kularatne et al.

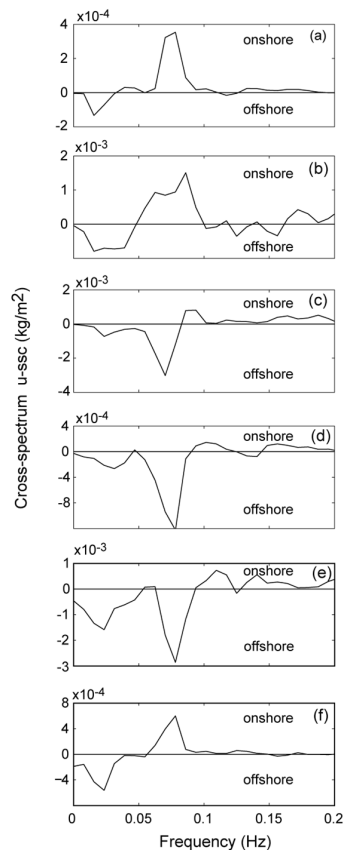


Fig. 14. Co-spectrum between the cross-shore current velocity (u) and suspended sediment concentration ($c_{0.05}$) at **(a)** site 2 at Port Beach1; **(b)** site 4 at Eagle Bay; **(c)** site 1 at Warnbro Sound; **(d)** site 2 at Safety Bay; **(e)** site 1 at Jurien Bay Jetty; **(f)** site 4 at south Pinnaroo.

Title Page

Abstract

Introduction

Conclusions

References

Tables

Figures

◀

▶

◀

▶

Back

Close

Full Screen / Esc

Printer-friendly Version

Interactive Discussion





Fig. 15. Collecting data over cross ripples, with primary and secondary ripples visible.

The effect of ripple types on cross-shore

S. R. Kularatne et al.

Title Page

Abstract

Introduction

Conclusions

References

Tables

Figures

◀

▶

◀

▶

Back

Close

Full Screen / Esc

Printer-friendly Version

Interactive Discussion

